Characterization of the interannual and intraseasonal variability of West African vegetation between 1982 and 2002 by means of NOAA AVHRR NDVI data

Nathalie Philippon, Lionel Jarlan, Nadège Martiny, Pierre Camberlin, Éric Mougin

Characterization of the Interannual and Intraseasonal Variability of West African Vegetation between 1982 and 2002 by Means of NOAA AVHRR NDVI Data

N. PHILIPPON
Centre de Recherches de Climatologie, UMR5210 CNRS, University of Burgundy, Dijon, France

L. JARLAN*
Centre d'Etudes Spatiales de la BIOsphère, UMR 5126 CNRS–UPS–CNES–IRD, Toulouse, France

N. MARTINY AND P. CAMBERLIN
Centre de Recherches de Climatologie, UMR5210 CNRS, University of Burgundy, Dijon, France

E. MOUGIN
Centre d'Etudes Spatiales de la BIOsphère, UMR 5126 CNRS–UPS–CNES–IRD, Toulouse, France

(Manuscript received 24 October 2005, in final form 29 August 2006)

ABSTRACT

The interannual and intraseasonal variability of West African vegetation over the period 1982–2002 is studied using the normalized difference vegetation index (NDVI) from the Advanced Very High Resolution Radiometer (AVHRR).

The novel independent component analysis (ICA) technique is applied to extract the main modes of the interannual variability of the vegetation, among which two modes are worth describing. The first component (IC1) describes NDVI variability over the Sahel from August to October. A strong photosynthetic activity over the Sahel is related to above-normal convection and rainfall within the intertropical convergence zone (ITCZ) in summertime and is partly associated with colder (warmer) SST in the eastern tropical Pacific (the Mediterranean). The second component (IC2) depicts a dipole pattern between the Sahelian and Guinean regions during the northern summer followed by a southward-propagating signal from October to December. It is associated with a north–south dipole in convection and rainfall induced by variations in the latitudinal location of the ITCZ as a response to the occurrence of the tropical Atlantic dipole.

The analysis of the intraseasonal variability of the Sahelian vegetation relies on the analysis of the seasonal marches and their main phenological stages. Green-up usually starts in early July and shows a very low year-to-year variability, while senescence ends by mid-November and is prone to larger interannual variability. Six types of vegetative seasonal marches are discriminated according to variations in the timing of phenological stages as well as in the greening intensity. These types appear to be strongly dependent on rainfall distribution and amount, particularly those recorded in late August. Finally, year-to-year memory effects are highlighted: NDVI recorded during the green-up phase in year j appears to be strongly related to the maximum NDVI value recorded at year $j - 1$.

1. Introduction

Vegetation is a key parameter in land–atmosphere interactions. As it is mainly climate driven, vegetation is highly sensitive to temperature and/or precipitation depending on the region considered [leaf area is larger in warm to hot areas with low light and high humidity than in sunny and dry environments or in cold climates; foliage emergence and senescence respond quickly to temperature increase and decrease in temperate climates while they are sensitive to rainfall and soil moisture in semiarid environments (Bonan 2002)]. Therefore, vegetation appears as a good marker for climatic disruptions. However, and retroactively, vegetation also affects climate over a wide range of spatiotemporal scales (Bonan 2002; Schwinning and Sala 2004) through

* Current affiliation: European Centre for Medium-Range Weather Forecasts, Reading, United Kingdom.

Corresponding author address: Nathalie Philippon, Centre de Recherches de Climatologie, UMR5210 CNRS, University of Burgundy, bât. Sciences Gabriel, BP 27877, 21078 Dijon CEDEX, France.
E-mail: nathalie.philippon@u-bourgogne.fr

DOI: 10.1175/JCLI4067.1

albedo, roughness, and soil moisture, which determine the partitioning of energy (Betts et al. 1996; Hutjes et al. 1998). The monitoring of vegetation is commonly performed using the normalized difference vegetation index (NDVI). This empirical index (Tucker 1979) is a function of absorbed radiation by chlorophyll in the red band and scattering by cellulose in the near-infrared (NIR). The NDVI is linearly related to the sunlit leaf area index (LAI) of the canopy and over vegetated land areas it usually ranges from 0.1 to 0.7 for low to high LAI.

West Africa has been subject to marked rainfall decreases over the last decades (Le Barbé et al. 2002, among others) and studies have revealed the importance of vegetation distribution and variability for monsoon and rainfall dynamics (Charney 1975; Eltahir and Gong 1996; Xue 1997; Zheng and Eltahir 1998; Zeng et al. 1999; Wang and Eltahir 2000a,b). However, relatively few studies that have examined vegetation (through NDVI) and climate relationships were specifically devoted to the West African region as a whole (Crépeau et al. 2003; Eklundh and Olsson 2003; Anyamba and Tucker 2005; Jarlan et al. 2005). Moreover, these few studies have given only a general picture of the rainfall and NDVI relationships over West Africa, and three major issues have not been comprehensively addressed yet.

The first issue is on the spatial patterns of interannual NDVI variability. Townshend and Justice (1986) and Dregne and Tucker (1988) noted a high spatial variability in the extension of the seasonal "green wave" from year to year (e.g., located farther south in 1984 than in 1983). Anyamba and Tucker (2005) provided yearly anomaly maps of NDVI over the Sahel. However, it is still not clear whether NDVI interannual variability organizes in coherent patterns across the subcontinent. Recently, Jarlan et al. (2005) extracted four modes of NDVI spatiotemporal variability by focusing on the Sahel region alone. During the core of the vegetative season, NDVI was shown to be highly correlated to the rainfall amounts recorded in the concurrent plus two previous months for the regions where less than 1000 mm are recorded (Malo and Nicholson 1990; Justice et al. 1991). Thus, the spatial patterns of NDVI anomalies partly resemble those of rainfall (Nicholson et al. 1990). However, any clear picture of joint modes of rainfall and NDVI variability over the region has never been provided. In particular, the phase locking of the interannual anomalies of NDVI with respect to the seasonal shift of the rainbelt is not well understood. Although specific patterns of NDVI variability can be extracted, it is not clear whether they are only locked to those of rainfall. They could also be partly dependent on the vegetation cover type.

Second, though West African rainfall is known to be related to sea surface temperature (SST) anomaly fields, no clear link between the latter (more particularly for the tropical Pacific) and NDVI has ever been demonstrated over West Africa until now (Anyamba and Eastman 1996; Myneni et al. 1996; Los et al. 2001 note that some of these studies were performed on periods less than 15 years long). Thus, little is known about the potential predictability of NDVI anomalies, even though it is important for impact studies and local communities. Only recently, Jarlan et al. (2005) identified significant lagged correlations between NDVI modes over the Sahel and various SST indexes over the tropical basins, suggesting some predictive potential.

A last issue is related to NDVI variability at the intraseasonal time scale. Although different recent studies aimed at detecting the phenological stages of the West African biomes (Crépeau et al. 2003; Zhang et al. 2005), none of them have ever explored the year-to-year variability in these stages. The first question is whether the year-to-year variability in green-up and senescence timing is related to the overall quality of the vegetative season. The second question is whether it is possible to identify typical seasonal marches of vegetation. The third question is how anomalies in the rainfall distribution impact the NDVI intraseasonal variability. Finally, we would like to address the question whether other factors play a role on seasonal phasing and also assess if seasonal phasing is important. For instance, recent studies argue for year to year memory in vegetation (Hiernaux et al. 1994; Schwinning et al. 2004; Martiny et al. 2005; Philippon and Fontaine 2002; Philippon et al. 2005).

Faced with the current growing scarcity of rain gauge data for Africa, NDVI data actually appear to be an attractive proxy of rainfall on small spatial scales (Myneni et al. 1996; Grist et al. 1997). The recent availability of corrected and intercalibrated long-term time series of NDVI on a 10-day time scale offers a unique opportunity to explore the above issues. These issues are of importance for several purposes, including climate modeling and vegetation as well as rainfall monitoring over West Africa and the Sahel. Section 2 gives a brief description of the data, including long-term (1982–2002) bias-corrected NDVI, rainfall, outgoing longwave radiation (OLR), and SST. Section 3 addresses the question of 1) the detection of the main modes of NDVI interannual variability by using the independent component analysis (ICA) and 2) their connections with climate variability. The ICA is a novel technique recently released in the field of geophysics.

TABLE 1. Characteristics of the different data used: Provider, spatial and temporal resolutions selected, domain, and period extracted.

Variable	Provider	Resolution		Domain	Period
		Spatial	Temporal		
NDVI[a]	ADDS	48 km	10 day and month	3°–18°N, 18°W–18°E	1982–2002
Rainfall	CRU[b]	0.5°	Month	4.5°–20°N, 20°W–20°E	1982–2000
	CPC[c]	2.5°	5 day	4.5°–20°N, 20°W–20°E	1982–2002
OLR[d]	CDC	2.5°	Month	5°S–25°N, 25°W–25°E	1982–2002
SST[e]	Met Office	1°	Month	40°S–40°N, 180°–180°	1982–2002

[a] http://igskmncnwb015.cr.usgs.gov/adds.
[b] http://www.cru.uea.ac.uk/~timm/grid/CRU_TS_2_0.html.
[c] http://www.cdc.noaa.gov/cdc/data.cmap.html.
[d] http://www.cdc.noaa.gov/cdc/data.interp_OLR.html.
[e] http://badc.nerc.ac.uk/data/hadisst/.

Particular emphasis is drawn on the spatial structures, the seasonal phasing, and the temporal evolution of these modes of variability. Their linkages and phasing with anomalies of precipitation, OLR, and SST fields are presented as well. Finally, section 4 is specifically devoted to the question of the intraseasonal variability of NDVI over the Sahel. A detection of the main phenological stages is proposed, and types of vegetative seasonal marches are also discriminated by considering variations in the timing of phenological stages and greening intensity. The factors governing the vegetative seasonal marches and phenological stages timing are discussed.

2. The datasets

a. The normalized difference vegetation index

The Advanced Very High Resolution Radiometer Normalized Difference Vegetation Index (AVHRR NDVI) dataset was downloaded from the Africa Data Dissemination Service Web site (ADDS; http://igskmncnwb015.cr.usgs.gov/adds). This Web site provides gridded time series of 10-day NDVI at 8-km spatial resolution over the period 1982–2003 for Africa only. This dataset has been processed by the Global Inventory Modeling and Mapping Studies group (GIMMS). Data are calibrated with respect to the NOAA satellite *NOAA-16* and SPOT VGT sensors and corrected for effects associated with aerosol contamination of the upper atmosphere and changes in viewing and illumination due to sensor degradation and orbital drift (Pinzon et al. 2004; Tucker 2005). Cloud contamination is reduced by a standard maximum value compositing technique (maximum value over the 10-day period attributed to the midpoint of the 10-day period). All of these corrections aim at reducing errors in the data. However, residual errors still remain.

For our purposes, we selected the West African window (3–18°N, 18°W–18°E), and spatially aggregated the data to a 48-km resolution (Table 1) by averaging pixels. First, this increases the signal-to-noise ratio and favors the detection of more coherent spatiotemporal modes of variability (Anyamba and Eastman 1996; Rigina and Rasmussen 2003). Second, this decreases the number of variables (cf. section 3a), leading to more robust patterns, and saves computing time. We retained the original 10-day time scale for the intraseasonal analyses but aggregated data to a monthly time scale for the interannual analyses.

b. Rainfall and OLR

Rainfall and OLR fields over West Africa were used as diagnostic variables for the NDVI variability. Rainfall data were extracted from (i) the Climate Research Unit (CRU) database for the interannual variability analysis and (ii) the Climate Prediction Center Merged Analysis Precipitation (CMAP) database for the intraseasonal analysis (Table 1). The Climate Research Unit rainfall dataset is a global gridded dataset of 0.5° spatial resolution and monthly time resolution, obtained by a direct interpolation from rain gauge records (Mitchell et al. 2004). Data cover the period 1901–2000. The CMAP dataset version selected is the merging of in situ rainfall measurements with satellite products (Xie and Arkin 1997). Its initial temporal and spatial resolutions are 5 days and 2.5° and the period is 1979–2003.

For regions where rainfall is strongly linked to deep convection, OLR data appears as a good indicator of the rainbelt location and convection intensity. Low OLR values are proved to signify deep convective clouds. The OLR data were obtained from the Climate Diagnostics Center Web site (http://www.cdc.noaa.gov/cdc/data.interp_OLR.html). It provides global interpolated OLR data over the period 1982–2005, on a

monthly time scale and at 2.5° spatial resolution (Liebmann and Smith 1996). We extracted the domain 5°S–25°N, 25°W–25°E (Table 1).

c. Sea surface temperatures

SST fields over the domain 40°S–40°N (Table 1) were used as an additional diagnostic variable for NDVI and its companion rainfall/OLR signals. We selected the First Hadley Centre Sea Ice and Sea Surface Temperature (HadISST1) dataset that combines monthly global fields of sea ice and sea surface temperature on a 1° space resolution from 1871 onward. Its improved interpolation procedure and the superposition of quality-improved gridded observations onto the reconstructions result in SST fields that show more uniform variance over time and better month-to-month persistence (Rayner et al. 2003) than those provided in the old version of the dataset [namely the Global Sea Ice and Sea Surface Temperature, version 2.3b dataset (GISSTv2.3b)].

OLR, SST, and CRU rainfall data were extracted over the period 1982–2000, while NDVI and CMAP rainfall data were extracted over the period 1982–2002 (Table 1).

3. Detection of the main modes of NDVI interannual variability over West Africa

a. The independent component analysis method

The identification of the main underlying modes of NDVI variability was achieved using the independent component analysis method (Hyvarinen and Oja 2000; Hyvarinen et al. 2001). ICA has recently been applied to geophysical fields and SST fields in particular (Aires et al. 2000, 2002; Lotsch et al. 2003). It has proven to be a powerful alternative to the common rotated principal component analysis (RPCA) methods. In ICA, data do not have to possess a Gaussian distribution (a rare feature in geophysical fields) and the components extracted are not simply uncorrelated but also statistically independent. Consequently, the tendency that underlies RPCA methods to mix several components, even when the signal is just their linear sum, is reduced with ICA. This is particularly obvious in our study: the RPCA method merges in a single mode, the first two modes (cf. section 3c) extracted by the ICA. For a full description of the method, readers are encouraged to refer to the publications cited above. In the current study, we ran the "FastICA" algorithm provided by the FastICA team of the Computer and Information Science Laboratory and Neural Networks Research Centre at Helsinki University of Technology (http://www.cis.hut.fi/projects/ica/fastica/).

TABLE 2. Cumulative percentage of explained variance (EV) by the first p principal components. Boldface indicates the number of PC retained for dimension reduction.

p	EV	p	EV
1	41	7	75
2	51	8	78
3	58	9	81
4	63	10	83
5	**68**	15	93
6	72	20	100

b. The NDVI data preprocessing

To show both the temporal (within a season) and the spatial covariability of NDVI, as well as to highlight possible latitudinal or longitudinal shifts in the course of the season, we organized the data matrix in a "temporal" and an "extended" form. Observations (in rows) are made up of years, while a given grid point for a given month stands for a distinct variable (in columns). Moreover, months were ordered from February to January to better match vegetative cycles. Such an extended matrix, already used with RPCA by Camberlin and Philippon (2002), is proved to be useful in depicting interannual and intraseasonal variability. However, due to the large number of variables (2129 grid points by 12 months) compared with the number of observations (21 yr), results are prone to be more unstable and the levels of variance explained are low. To ensure the robustness of the modes, we carried out a series of experiments where (i) data are detrended, (ii) different numbers of modes are considered for data dimension reduction (Table 2), or (iii) data are kept with their original 10-day and 8-km spatiotemporal resolution (Table 1). In all these experiments, similar modes were obtained.

Two types of preprocessing were applied to the matrix before running the FastICA algorithm. First, data were centered by removing the seasonal cycle, that is, the corresponding monthly mean is subtracted from each grid point and month over the entire 21-yr period. Data were not normalized by the standard deviation so that the errors, which characterize NDVI for low vegetated pixels, have small effects on the analysis. No other processes, such as filtering or detrending, have been applied. Indeed, a homogeneity test performed at the gridpoint scale (not shown) did not reveal any abrupt shift in the time series. In addition, over the study period a positive trend in rainfall amounts over the Sahel is observed (Eklundh and Olsson 2003; Nicholson 2005). This rainfall trend gives a physical basis to the trends that could be observed in NDVI. Second, noise as well as matrix dimensions are reduced by using a principal component analysis. Following the

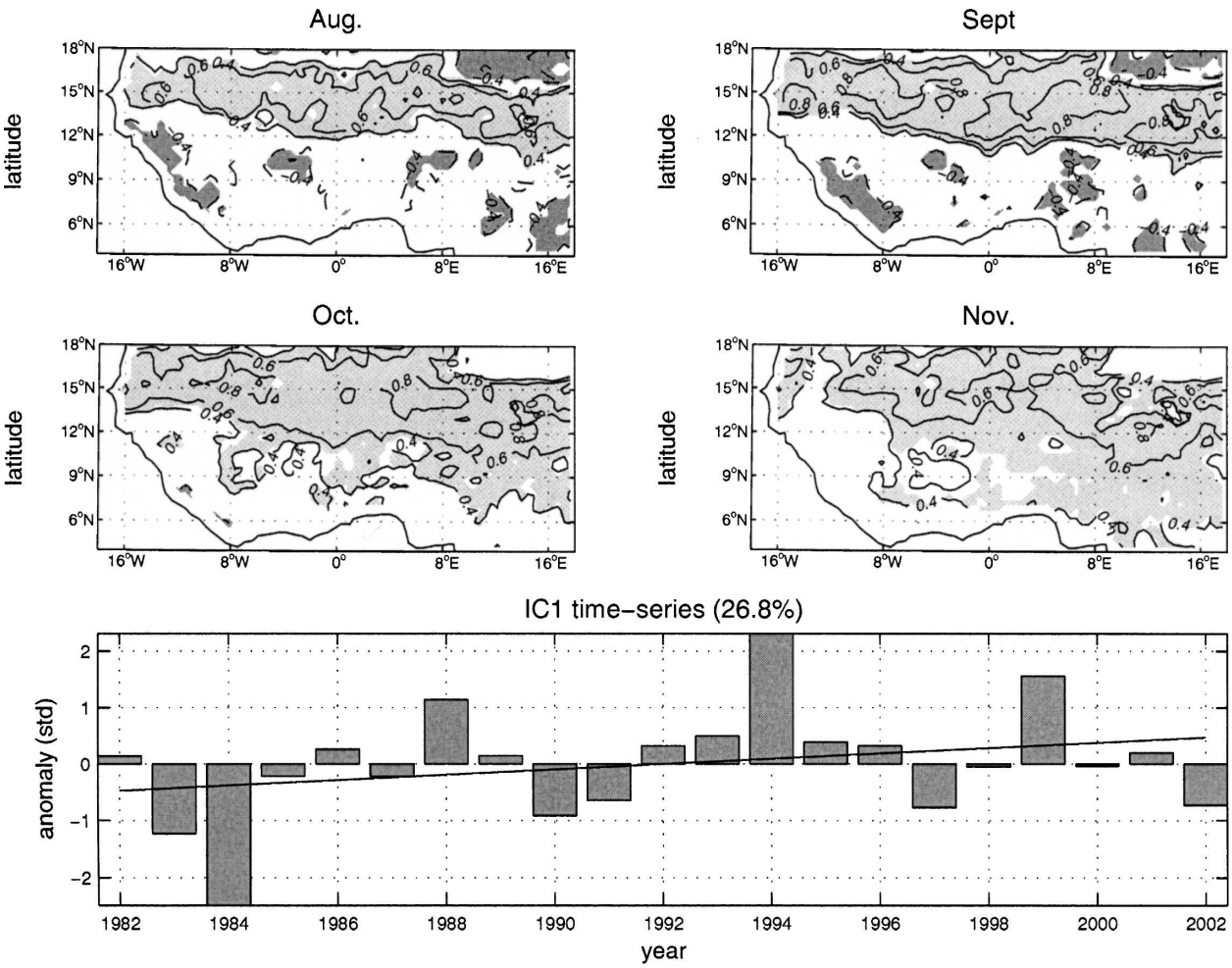

FIG. 1. (top) Correlation maps of the first independent component (IC1) time series with August to November NDVI fields. Solid (dashed) lines enclose positive (negative) correlations above 0.4 (below −0.4). Shading indicates statistical significance at the 95% level over 1982–2002. (bottom) IC1 standardized time series and its linear trend and, in parentheses, the variance explained.

scree-slope criterion (Wilks 2006), only the first five principal components (PCs) are retained. They explain ~68% of the total variance (Table 2).

c. *Resulting leading independent components*

Among the first five independent components retained, only the first two (IC1 and IC2) are displayed (Figs. 1 and 2, respectively). They are described by a yearly time series and a series of monthly maps showing the correlations between the time series and the NDVI monthly fields. We only display monthly maps that present the highest statistically significant correlations (95% level).

The first component (IC1, Fig. 1) explains 26.8% of the total variance. This can be considered as the "Sahelian" mode. It mainly captures the NDVI variability over the Sahel from August to October. In September (i.e., during the peak of photosynthetic activity) a very distinct band appears between latitudes 13° and 18°N, with a slight northwest–southeast tilt, consistent with vegetation and precipitation distribution. In October, the signal spreads southward. From November, it weakens and its spatial coherence fades away. According to the global land cover classification for the year 2000 (GLC2000; Africa map Mayaux et al. 2004), this Sahelian mode encompasses from north to south the domain of open grasslands to open deciduous shrublands where herbaceous cover accounts for 80%–50% of the total vegetation cover. In the south Sahel shrublands are mixed with crops (representing up to 30% of the cover in some places), while in the north Sahel bare soil dominates (Hansen et al. 2002). Thus, IC1 includes vegetation with very different physiognomic characteristics that, nonetheless, share a common interannual variability in photosynthetic activity. The IC1 time series is characterized by the anomalous low (high) photosyn-

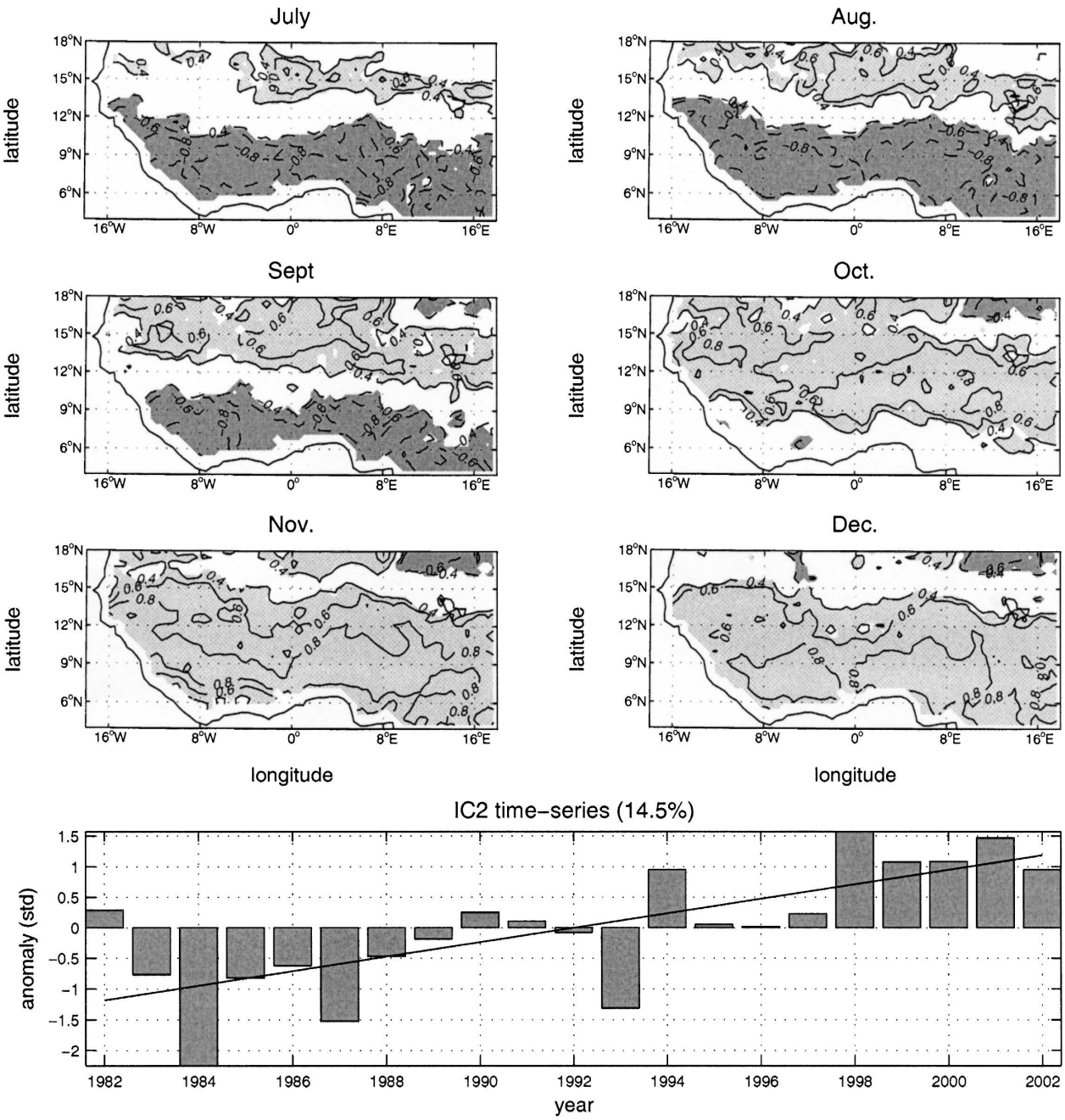

FIG. 2. As in Fig. 1, but for the second independent component (IC2) and the months of July to December.

thetic activity years of 1983–1984–1990–1997–2002 (1988–1994–1999). According to the Spearman rank correlation (Wilks 2006), the IC1 time series positive trend is not significant at the 95% level. This result is obtained for a large region and is not contradictory with those found by Eklundh and Olsson (2003), Olsson et al. (2005), and Anyamba and Tucker (2005). At pixel scale, significant positive trends are observed in particular over the eastern part of the Sahelian belt (i.e., east of 20°E, a region not considered in this study).

Two interesting signals are depicted in the second component (14.5%, Fig. 2). The first signal is dipole-like. It opposes, during summertime (i.e., July–August), the central Sahel and the Guinean region, which experiences its minor dry season at this time. Indeed, the intertropical convergence zone (ITCZ) is located at its

northernmost position (mean latitudinal location of the maximum rainfall values around 10°N). However, correlations are higher over Guinea. The second signal consists of a southward propagation from October to December of the NDVI anomalies observed in the summer over the Sahel. Therefore, for the region south of 12°N, the July–September and November–December periods show opposite variations (i.e., when summer is more active than average, autumn is less average). In fact, this mode depicts a change in the phase of the seasonal cycle over the Guinean region. According to IC2 time series, these dipole patterns (and propagation signals) were most pronounced in 1984, 1987, 1993, 1998, and 2001. They are obvious from the NDVI anomaly maps provided by Anyamba and Tucker (2005) for the years 1987, 2000, 2001, and 2003. Additionally, IC2 time series presents a positive and strongly significant trend. This suggests that, over the last two decades, vegetative activity became stronger (weaker) over the central Sahel (Guinea coast) in summer and also longer over the Sudanian region. Tateishi and Ebata (2004) studied phenological changes at the near-global scale between 1982 and 2000. The West African pixels are divided between the 7th and the 11th class characterized by increasing trends of NDVI peak level and vegetative cycle duration, respectively. The IC2 time series trend, and to a lesser extent that of IC1, agrees with those highlighted for rainfall in previous studies: Nicholson et al. (2000) and Dai et al. (2004) have shown that Sahelian rainfall has somewhat recovered since the 1990s, even if the average remains below the pre-1970 mean. Last, like IC1, IC2 spatial patterns encompass different ecosystems. The Guinean pole observed in July–September is the domain of deciduous shrublands and woodlands, with tree cover ranging from 20% to 70%.

Finally, among the five ICA modes obtained, most of them mainly capture the summer to autumn NDVI variability. Indeed, vegetative activity is the strongest during these seasons. The NDVI variability related to vegetation senescence is only depicted in two components (IC2 and IC5, the latter not shown) as a southward-propagating signal in autumn, whereas no component depicts the one associated with the green-up, frequently referred to as the green wave. This could be explained by their different latitudinal shift rates: 0.12 days km^{-1} for green-up compared to 0.05 days km^{-1} for senescence according to Zhang et al. (2005).

d. Independent components linkages with atmospheric fields

To assess the links between the two NDVI ICA modes and the regional climate, we performed a composite difference analysis (Von Storch and Zwiers 1999) on rainfall and OLR fields averaged over 20°W–20°E and considered from April to December and from 2.5° to 22.5°N. Years of low (high) photosynthetic activity were defined as those recording an NDVI anomaly lower (higher) than −0.5 (0.5) standard deviation over the period 1982–2000. The significance of the results (95% level) was tested with a Student's *t* test (Von Storch and Zwiers 1999).

Results of the rainfall and OLR composite analysis for IC1 are displayed in Figs. 3b,c as time–latitude diagrams. We also provide results for NDVI (Fig. 3a). However, note that NDVI patterns from the composite analysis can be somewhat different from those of the ICA. Indeed, the composite analysis relies on samples of years and the period considered is 1982–2000 instead of 1982–2002, since CRU rainfall data are documented for the former period only. The mean annual cycle for each variable is also displayed as black thin lines. The years when IC1 shows "low" and "high" photosynthetic activity are 1983–1984–1990–1991–1997 and 1988–1994–1999, respectively. The composite analysis indicates that more intense photosynthetic activity over the Sahel [from August to October (Figs. 1 and 3a)] is associated with higher July to September rainfall amounts from 10° to 17.5°N (Fig. 3b) and lower OLR values from 10° to 22.5°N, indicative of deeper convection (Fig. 3c). This agrees with the 1-month lag that exists in the rainfall–vegetation relationships over the Sudanian–Sahelian regions (Malo and Nicholson 1990; Nicholson et al. 1990; Justice et al. 1991; Shinoda 1995). The differences between the two samples of years are large for the three fields: up to 0.1 unit of NDVI, 100 mm, and 16 W m^2 at the core of the vegetative and rainy seasons (September and August, respectively). The rainfall and OLR largest differences are located just at the northern edge of the ITCZ mean location (12.5°–15°N, Figs. 3b,c). This suggests that convection is more intense within the ITZC, which also covers a wider area.

Results for IC2 are displayed in Figs. 3d–f. The years used to perform the composite analysis are 1987–1993–1996 (1982–1990–1998) for which detrended IC2 anomalies are lower (higher) than −0.5 (0.5) standard deviation (σ) and IC1 anomalies are lower than 0.5 σ in absolute value. The years 1984 and 1994 for which both IC1 and IC2 record strong anomalies are therefore excluded. This highlights the specificities of the patterns related to IC2, but, on the other hand, it also partly weakens the signal and leads to lower difference values. The Sahel–Guinea dipole observed from July to September in IC2 (Fig. 2) appears in the rainfall and OLR patterns. Lower (higher) photosynthetic activity over

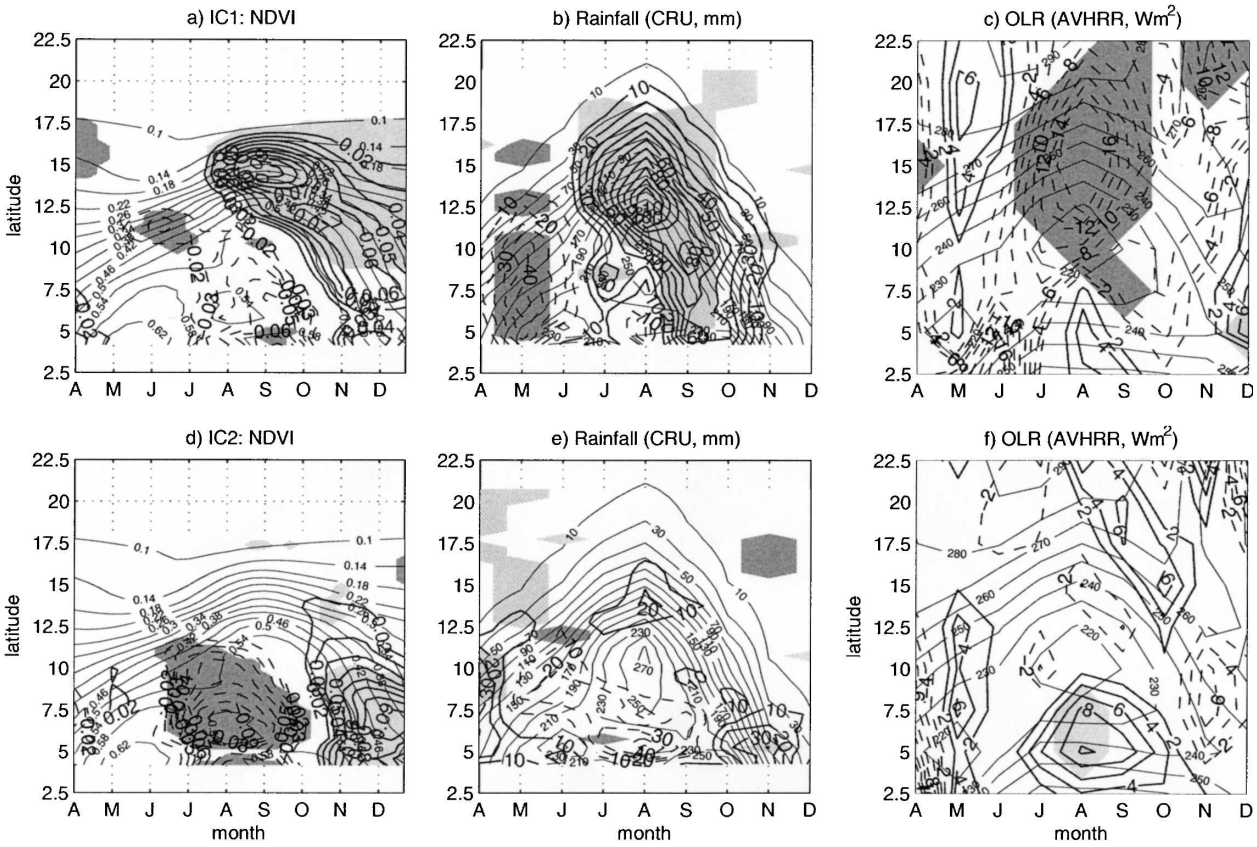

FIG. 3. Time–latitude diagrams (from 2.5° to 22.5°N and April to December) of composite differences of NDVI (unitless), rainfall (from CRU dataset, mm), and OLR (W m^2) averaged over 18°W–18°E with respect to years of high minus low NDVI for (a)–(c) IC1 and (d)–(f) IC2. Solid red (dashed blue) lines enclose positive (negative) differences. Shading indicates differences significant at the 95% level according to a Student's *t* test. Black solid lines display the mean annual cycle.

Guinea (the central Sahel) is associated with below (above)-normal rainfall amounts south (north) of 12°N (Fig. 3e) and decreased convection south of 10°N (Fig. 3f). July–August over Guinea corresponds to the minor dry season. Thus, the patterns of rainfall and OLR associated with IC2 feature variations in the latitudinal position of the ITCZ rather than variations in convection intensity as compared to those associated with IC1. Difference values are higher (and significant) for the Guinean pole than for the Sahelian pole, which does not appear anymore in the NDVI composite diagram (Fig. 3d). As already mentioned, this is due to the small number of years used in the composite and also to the spatial average performed over longitudes 18°W–18°E. Finally, the southward spread of the NDVI anomalies from October to December (Figs. 2 and 3d) can be related to above-normal rainfall amounts recorded during the rainbelt withdrawal, and in particular during the second rainy season over Guinea (Fig. 3e).

The unexpected result of this study is the extraction of a NDVI dipole mode that matches the well-known rainfall dipole (Janicot 1992). This implies a role played by the minor dry season on Guinean vegetation photosynthetic activity.

e. Independent component linkages with SST fields

As a complementary diagnostic, we performed a composite difference analysis on bimonthly sea surface temperature fields considered between 40°S and 40°N (Fig. 4).

May–June, July–August, and September–October SST composite maps relative to IC1 are provided in Figs. 4a–c. A higher photosynthetic activity over the Sahel from August to October is primarily associated with (i) negative SST anomalies in the tropical eastern Pacific (i.e., a "La Niña" event) and (ii) positive SST anomalies in the Mediterranean. Anomalies appear as early as May, but they are mainly significant during summertime for the two basins. Anyamba and Eastman (1996) and Myneni et al. (1996) could not draw any clear conclusions regarding the Sahel by analyzing the NDVI variability over Africa and its link with ENSO.

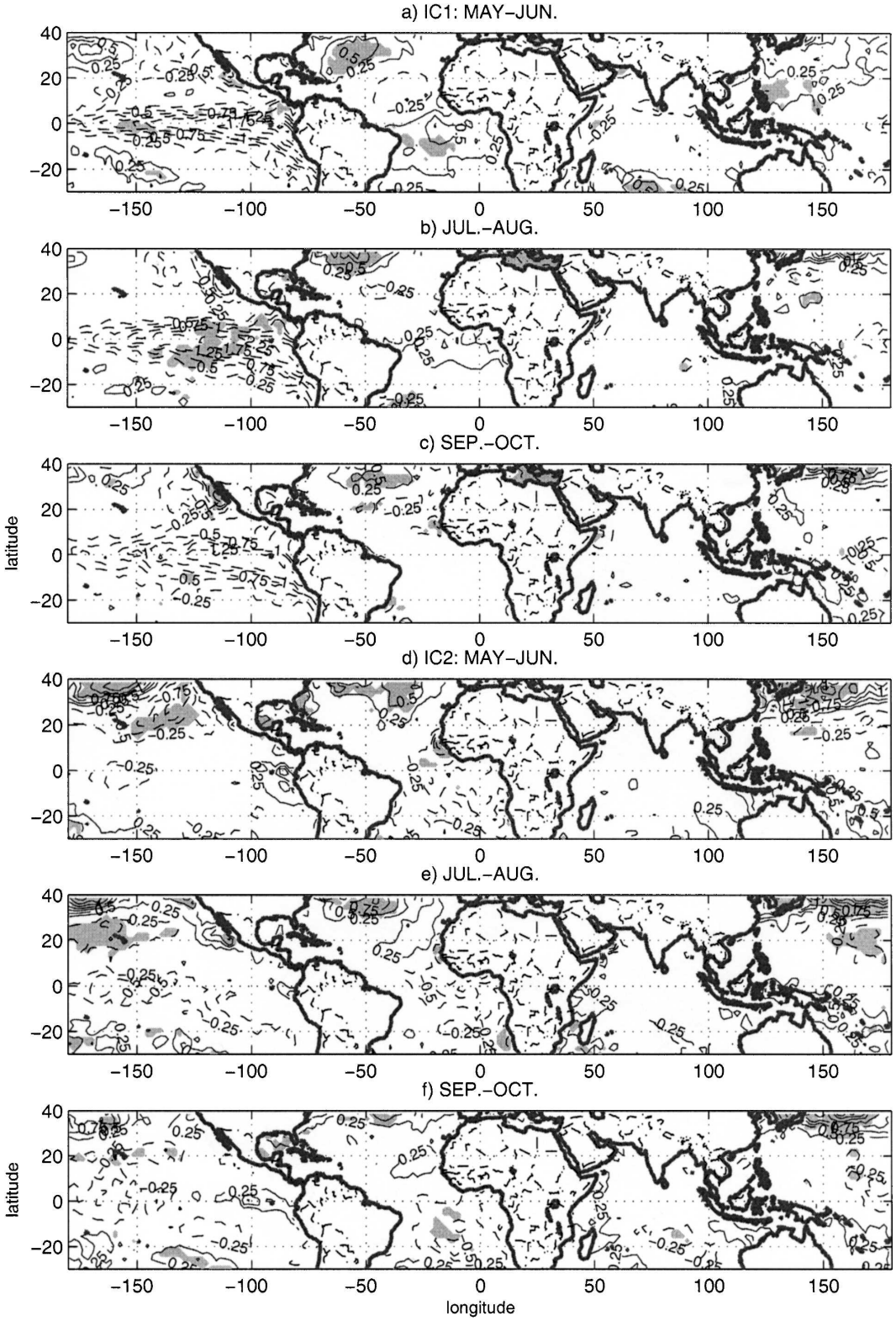

FIG. 4. Bimonthly maps of composite differences of sea surface temperature fields with respect to years of high minus low NDVI (see text for details) for (a)–(c) IC1 and (d)–(f) IC2. Solid (dashed) lines enclose positive (negative) differences. Shading indicates differences significant at the 95% level according to a Student's *t* test.

However, the sample of years that they used was limited (1986–90 and 1982–90, respectively). Our results support previous studies linking global SST and Sahelian rainfall variability and demonstrating

- an enhanced impact of the ENSO phenomenon on Sahelian rainfall from the 1980s onward (Janicot et al. 1996): The teleconnection is indirect and involves a modification of the zonal pressure gradient between the eastern Pacific and the Atlantic tropical basins. This gradient modulates the trade winds and the moisture advection strength over West Africa (Camberlin et al. 2001; Janicot et al. 2001). Rowell (2001) also notes a direct atmospheric teleconnection via Kelvin and Rossby waves interacting above West Africa to enhance large-scale subsidence over the Sahel. In the case of a cold event (as depicted by our maps), the pressure gradient is decreased and trade winds and moisture advection are strengthened.
- a significant role played by the Mediterranean: The latter directly impacts moisture advection to West Africa from the north (Raicich et al. 2003) and indirectly moisture convergence and the hydrological cycle through feedbacks between convection and the local atmospheric circulation (Rowell 2003). When warmer conditions prevail in the Mediterranean, moisture advection, moisture convergence, and the hydrological cycle are enhanced. It has been recently demonstrated that the variability of the Sahelian rainfall is also driven by SST variability in the tropical Indian Ocean (Bader and Latif 2003; Giannini et al. 2003). No coherent and significant signal appears in this study over this basin. However, this is merely attributed to our study period that is restricted to the recent two decades, which does not capture long-term decadal variability.

On the whole, the SST patterns associated with a IC1 positive anomaly lead to a general intensification of convection within the ITCZ, a northward shift of its northern edge, and a rainfall increase. This is in agreement with signals obtained in the OLR and rainfall composite diagrams (Figs. 3b,c).

Figures 4d–f provide SST composite maps for IC2 (based on detrended time series). The most interesting signals are found over the tropical Atlantic basin. The dipolar NDVI pattern seems associated with the occurrence of the "tropical Atlantic dipole" (Servain 1991), showing a colder south tropical Atlantic and a warmer north tropical Atlantic when the photosynthetic activity over the Guinean coast (the central Sahel) is low (high). Such a SST pattern increases the meridional temperature gradient between the Gulf of Guinea and West Africa and therefore induces a stronger monsoon. The ITCZ is usually located northward, and a dipole rainfall pattern develops over West Africa (Fontaine and Janicot 1996; Fontaine et al. 1998; Vizy and Cook 2001 among others; see also Figs. 3e,f). The maintenance of the tropical Atlantic dipole in September–October contributes to a slowdown in monsoon withdrawal. It is accompanied by larger rainfall amounts in October–November over Guinea (Fig. 3e), which contributes to an enhancement of the photosynthetic activity (Fig. 3d). Once again, SST anomalies precede those of NDVI by at least two months, indicating that NDVI is potentially predictable from SST. Jarlan et al. (2005) even found significant 9-month lagged relationships between Sahelian modes of NDVI and the interhemispheric SST gradient over the Atlantic.

4. Characterization of variability in vegetation phenology over the Sahel

The FastICA applied in an extended form provided us with information on the intraseasonal variability of NDVI. However, it did not allow us to precisely characterize the course of the vegetative season, particularly its main phenological stages, and associated variability. These points are examined for the Sahel based on a Sahelian NDVI index computed according to the FastICA results: this is done by averaging the September grid points significantly correlated at the 95% level to the IC1 time series (i.e., those contained inside the 0.4 contour line on the September map in Fig. 1). This index documents the area extending from 13°–18°N and 18°W–18°E. Its correlation with the IC1 time series gives a coefficient of 0.92 when taking the average over August–October. An analysis of the index time series (raw data) revealed erroneous data from October to December 2002. Consequently, we restricted the study period to 1982–2001 in the following analyses.

a. Main stages of vegetation phenology over the Sahel

The NDVI mean seasonal cycle over the Sahel is presented in Fig. 5 (shaded bars) as departures from the annual mean ($\bar{x} = 0.21$). We defined the vegetation green-up (senescence) date as the 10-day period that precedes the one when NDVI reaches up (down) to the annual mean level (Fig. 5, level "0"). Thus, we mainly extracted the limits of the highest photosynthetic activity period and not the actual onsets of vegetation green-up and senescence. This simple method provides the same results as those obtained using the method of Tateishi and Ebata (2004) or Camberlin and Diop

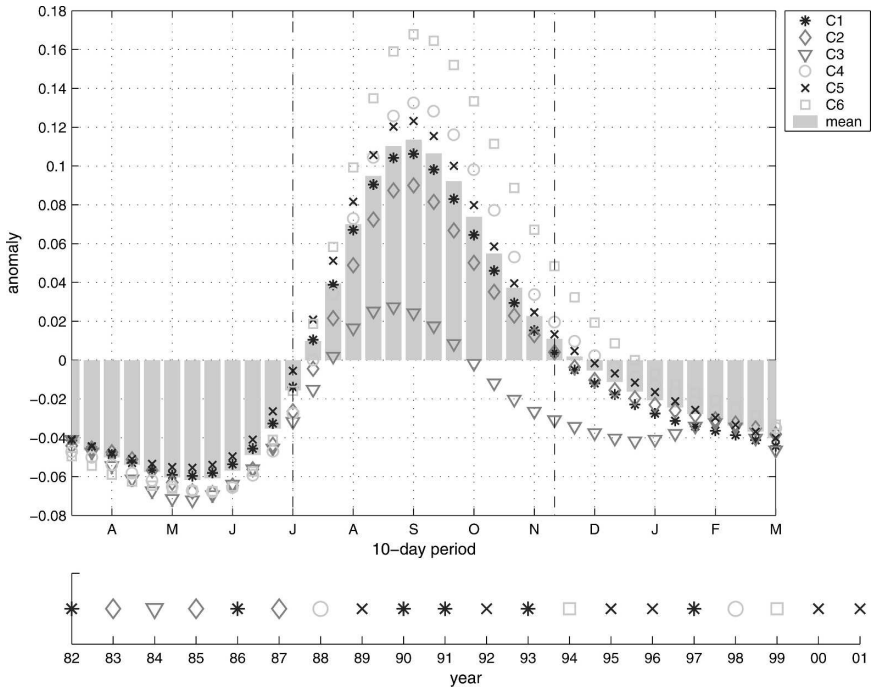

FIG. 5. (top) Mean seasonal cycles, expressed as departures from the 1982–2001 annual mean ($\bar{x}$ = 0.21) of the Sahelian NDVI. Shaded bars display the 20-yr mean cycle, while markers display the mean cycle for each of the six classes as determined from a cluster analysis. Dash-dotted lines mark median onset and cessation dates of the high photosynthetic activity period. (bottom) Distribution of the six classes over the study period.

(2003) based on computation of slopes for three consecutive 10-day periods or on cumulative anomalies. The main characteristics of Sahelian vegetation phenology are summarized in Table 3.

The median date for the onset of high photosynthetic activity is the first 10 days of July. This date, hereafter referred to as the onset date (OD), is in agreement with the dates obtained for a Sahelian pixel by Moulin et al. (1997), as well as with those mapped for the whole West Africa by Crépeau et al. (2003) and the Sahel by Zhang et al. (2005). These maps highlight a substantial lag between the OD at the southern and the northern parts of the region (end of May versus mid-July). The onset of high photosynthetic activity can be related to the monsoon arrival over the region. The OD follows the ITCZ northward shift (Sultan and Janicot 2000; Louvet et al. 2003) by about 1 to 2 weeks. This shift clearly appears in Fig. 6, which displays differences between the rainfall field at the OD and the rainfall field at OD minus two 10-day periods: the Sudanian and Sahelian regions experience a rainfall increase while a decrease is observed over Guinea. The rapid growth response to the early rains is characteristic of savanna grasslands. Herbaceous germination and growth only require shallow infiltration in the upper soil layer and react rapidly even to small and short rainfall pulses (Akpo and Grouzis 1993; Schwinning and Sala 2004). The OD shows weak interannual variations. Its standard deviation is 5.2 days and agrees with the standard deviation obtained by Tateishi and Ebata (2004). Field observations suggest that a greater interannual variability is observed at green-up; herbaceous germination can occur between early June and mid-July. However, germination is associated with rainfall events that are very irregular in space and time and with low densities of

TABLE 3. Median dates, standard deviations, and trends over the period 1982–2000 of the main phenological stages of the Sahelian vegetation index. Last column: correlation between the dates of phenological stages and August to October NDVI (detrended within parentheses). One (two) asterisks denote coefficients significant at the 95% (99%) level, and # denotes low and nonsignificant Spearman correlation coefficients.

	Date (10-day period, as from January)	Std dev (10-day period)	Trend (Spearman correlation)	R_{ASO} (detrended)
Onset	19	0.52	#	−0.42* (−0.21)
Cessation	32	1.99	+0.65**	0.91** (0.90)
Peak	25	0.48	#	0.39
Length	13	2.24	+0.66**	0.91**

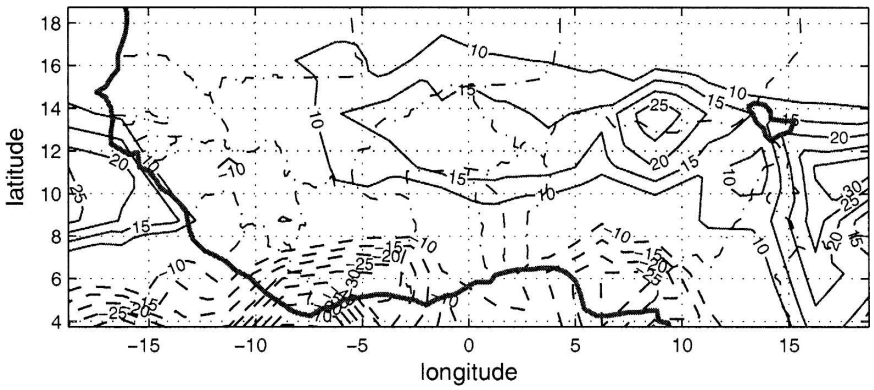

FIG. 6. Difference map of the rainfall field (from CMAP) at OD and OD minus two 10-day periods. Solid (dashed) lines display positive (negative) differences above 10 mm (below −10 mm).

vegetation. As a consequence, vegetation development at germination cannot be detected by the sensors. Rather, our onset date corresponds to the time when the herbaceous cover is large enough, in relation to a monsoon well settled over the region (Fig. 6), accompanied by more regular rainfall events and higher rainfall amounts and soil wetness. Finally, OD time series does not show any trend or robust association with August–October NDVI anomalies. The OD of the high photosynthetic activity period does not seem to determine the quality of the following vegetative season.

The cessation of the high photosynthetic activity period (referred to as CD hereafter) occurs during the second 10-day period of November. This is also consistent with results from Crépeau et al. (2003). However, field observations by Akpo and Grouzis (1993) indicate that most of the vegetation is dry as early as in mid-October (e.g., 70% of dry matter by mid October in 1990 in the Ferlo grasslands, around 14.5°N in Senegal). This one month difference between observations and our computation could rely on several factors. First, it is certainly due to the size of our NDVI index. This index encompasses southern regions characterized by higher tree densities. De Bie et al. (1998) noted that the leaves of deciduous trees do not fall immediately at the end of the rainy season but only once they are dry. Thus, several phenological behaviors are merged in our index. Second, as compared to the abrupt decrease of rainfall by September, the NDVI decrease is smoothed. This is particularly noticeable by mid-October when the slope becomes less sharp. This characteristic is thought to be due to the presence of (i) dust aerosols and (ii) bare soils at this period of the year. The brightness and color of bare soils and the amount of aerosols are responsible for NDVI variability, which can be even higher than the one actually due to vegetation itself (Huete and Tucker 1991; Hanan et al. 1995). However, we think that the one-month deviation of our cessation date from observation is minor and does not affect the relative variations for the purpose of studying interannual variability. As compared to the OD (Table 3), CD shows larger interannual variations. Its standard deviation is about 20 days. The CD is also characterized by a significant rising trend. Spearman's correlation coefficient is equal to 0.65, significant at the 95% confidence level. This trend suggests an extension of the vegetative season with time. It is also related to the increased summer rainfall amounts recorded in the last years over parts of the Sahelian region (Nicholson 2005). The CD is strongly linked to the quality of the vegetative season. A correlation coefficient of 0.91 (remaining as high as 0.89 when both time series are detrended) is obtained between August–October NDVI and the CD time series. Finally, the median length of the vegetative season is thirteen 10-day periods (i.e., about 4 months). The peak in photosynthetic activity occurs during the first 10 days of September and is very stable (Table 3). The minimum (recorded in May) is likely ascribable to signal contamination by high levels of aerosols and water vapor (Nicholson et al. 1990; Tanré et al. 1992; Holben et al. 2001) rather than to an actual phenological stage.

b. Year typing

The next step aims at detecting specific seasonal courses of vegetation. To that end, the NDVI seasonal cycles for the 20 years between 1981 and 2001 were expressed as departures from the annual mean and organized from the second 10-day period of March in year i to the first 10 days of March in year $i + 1$. A cluster analysis was applied to these cycles. Ward's method was chosen, based on inner squared distance, to find homogeneous clusters. Six distinct classes were identi-

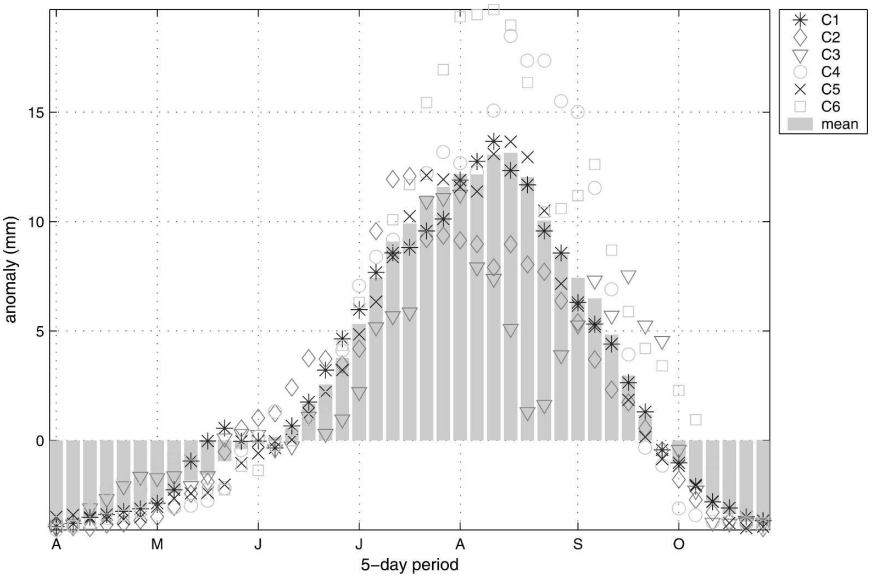

FIG. 7. As in Fig. 5 top panel but for April to November 5-day rainfall amounts from CMAP (x = 4.4 mm).

fied by scrutinizing the hierarchical cluster tree. They are composed of 6, 3, 1, 2, 6, and 2 yr, respectively. Results are presented in Fig. 5 where the mean annual cycle for each class (markers) is superimposed on the mean annual cycle computed with all the observations (shaded bars).

Classes 1 and 5 (Figs. 5, C1, and C5 represent years for which the photosynthetic activity course and level are close to average. Compared to Class 5, Class 1 records a slightly below normal vegetative activity that also ends earlier. Classes 2 and 3 (Fig. 5, C2, and C3) are representative of years of low photosynthetic activity. They show a delayed green-up and a slower vegetation growth (gentle upward slopes). The year 1984, which in itself composes the third class, is exceptional. The vegetative season lasted only 2 months (as compared to a median of 4 months) from mid-July to the beginning of October. Moreover, the NDVI maximum recorded is as low as 0.24, suggesting very weak primary production. Classes 4 and 6 correspond to years of high photosynthetic activity (Fig. 5, C4, and C6) and feature a longer season and a more acute vegetation growth. The NDVI maximum for type 6 reaches 0.38.

The classes picture strong differences in terms of peak intensity but small differences in the timing of the peak (cf. low peak standard deviation in Table 3). Classes 4 and 5 present close peak levels, but for Class 5 vegetation growth starts earlier. Class 5 year usually follow the wettest years of 1988, 1994, and 1999 (C4 and C6, Fig. 5, bottom panel). This suggests that the rainfall conditions of the previous year could influence vegetation growth during the following year. This question is explored in the next section. Last, the bottom panel in Fig. 5 indicates that years of low (high) vegetative activity preferentially occurred during the 1980s (1990s). This is in agreement with the positive trends observed in the IC1 and IC2 time series (Figs. 1 and 2).

c. *Potential factors governing interannual variations in vegetation phenology*

The objective of this section is to document the causes of the vegetation seasonal march variability. Previous studies have demonstrated that rainfall is the dominant climatic factor that controls NDVI variability at tropical latitudes. Using the CMAP rainfall dataset at the 5-day (pentad) time resolution, we computed the rainfall marches associated with the six specific vegetation marches highlighted in the previous section (Fig. 5). These mean rainfall courses were filtered using a 15-day moving average. Results are presented in Fig. 7. As in Fig. 5, shaded bars give the 20-yr mean annual course, and markers show the mean annual course for each of the six classes. The differences between years of low and high photosynthetic activity concern the rainfall amounts and the rainy season phase. Years of low (high) photosynthetic activity (C2 and C3 versus C4 and C6) are usually associated with large rainfall deficits (excess), particularly at the end of August, so that the rainfall seasonal cycle peak seems to be shifted toward July (September). Thus, the rainfall distribution during the season is as important as rainfall amounts for vegetation growth, and rainfall amounts recorded at the

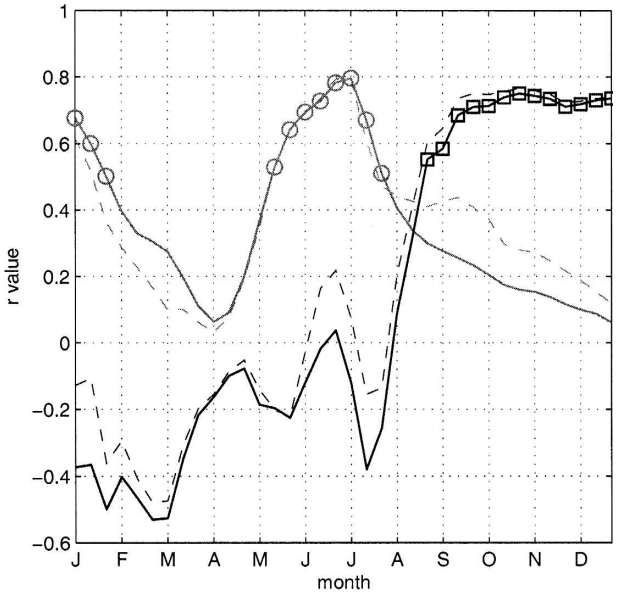

FIG. 8. Total correlation coefficients between 10-day NDVI of year j and (a) rainfall (from CMAP) accumulated since the beginning of year j (black solid line) and (b) NDVI maximum value of year $j - 1$ (gray solid line, see text for details). Markers denote 10-day periods for which the correlation is significant at the 95% level. Partial correlation coefficients are displayed as dashed lines.

end of August appear to be the most crucial in determining the overall quality of the vegetative season. Sequences of consecutive dry spells usually lead to vegetation growth failure. For instance, in 1984 (C3), anomalies in August rainfall amounts were very pronounced. Added to marked successive deficits during the first five pentads of July, these anomalies contributed to the early collapse of the vegetative season, despite the return to positive rainfall anomalies in mid September.

The sensitivity of vegetation growth to rainfall accumulated in the course of the rainy season is further explored and quantified through correlation analysis. The thick black line in Fig. 8 provides correlations between NDVI of a 10-day period i of year j and rainfall accumulated since the beginning of year j (squares denote significant correlations at the 95% level). Given the fact that, over the region, the first rains usually occur in June and the last rains are recorded in late September, attention must be mainly paid to June–September correlations. Interestingly, there is virtually no significant relationship between accumulated rainfall and NDVI before mid August. By September (i.e., the core of the vegetative season) the relationships become significant, but variations in rainfall accumulated until then are far from fully contributing to NDVI variability (about 50% of variance explained only). The sustained high correlations after the end of the rainy season are mainly due to strong persistence effects in NDVI [see Fig. 1, which shows a persistence of the signal until November, as well as Philippon et al. (2005)]. Note that the Sahelian NDVI averaged over August–October correlates at 0.64 with rainfall amounts recorded during the last 10 days of August. Thus, the underlying question is what are the other factors that control NDVI in the course of the vegetative season?

As observed in Fig. 5, years with abnormally high NDVI levels in May–June (C5) follow years with the highest NDVI levels and the longest vegetative season (C4 and C6). Martiny et al. (2005) noted that the annual NDVI level is not only highly dependent on the rainfall amounts of the concurrent year but also on that of the previous year. Given the fact that upper soil moisture anomalies over the Sahel disappear two months after the beginning of the dry season (Shinoda and Yamaguchi 2003), such an interseason memory is thought to pass through vegetation itself, in particular through roots, seeds, and foliation (Schwinning et al. 2004). For example, Hiernaux et al. (1994) observed for the Sahel that tree foliation of one given year depends on the quality of the previous rainy season. These interseason memory effects are explored by computing correlations between NDVI of a 10-day period i of year j with the maximum NDVI value of the year $j - 1$. This value is representative of the quality of the vegetative season. Results are presented in Fig. 8 as the full gray line. An unexpected result is that the quality of the past year vegetative season seems to impact on NDVI in June rather than during the core of the vegetative season. June is the time of the actual green-up of woody vegetation over the region. Tree foliation occurs before the first rain (de Bie et al. 1998) and herbaceous and woody covers in savannas present asynchronous behavior in terms of biological activity (Fontès et al. 1995). Thus, these results are in agreement with the study by Hiernaux et al. (1994). Partial correlations computed independently from current year accumulated rainfall (gray dash line) indicate that about 16% of NDVI variability is still explained by the quality of the past year vegetative season during its core period. This is also coherent with findings by Schwinning et al. (2004) and Martiny et al. (2005) for subarid regions of North America and tropical Africa, respectively.

5. Summary and conclusions

This paper aimed at providing a detailed picture of the interannual and intraseasonal variability of the vegetation photosynthetic activity over West Africa over the last 20 years through analysis performed on normalized difference vegetation index (NDVI) data.

The first set of analyses was dedicated to the extraction of the main modes of NDVI interannual variability. To this aim, we used the recently developed independent component analysis technique and applied it to an extended matrix in order to assess the temporal (month to month) and spatial coherence of NDVI variability. A climatic interpretation of the detected modes was then performed based on composite analysis of ocean–atmospheric fields. Two dominant modes of NDVI variability could be linked to well-known patterns of rainfall, OLR, and SST anomalies:

- First, a "Sahelian" mode depicting the NDVI variability from August to October over the region 13°–18°N, 18°W–18°E. Years of high photosynthetic activity are usually characterized by above-normal rainfall and deep convection at summertime over a broad Sudanian–Sahelian band while the eastern tropical Pacific (Mediterranean) exhibit negative (positive) temperature anomalies. These SST patterns were proved to favor a more intense convection at the ITCZ mean location.
- Second, a "dipole" mode featuring opposed variations between the Sahel and Guinea at summertime. Years with a positive (negative) NDVI pole over the Sahel (Guinea) experienced comparable patterns in rainfall and OLR, as well as a north–south SST dipole in the tropical Atlantic.

The time series of both modes exhibit positive trends between 1982 and 2002 in agreement with observations made on rainfall amounts. This supports previous reports arguing for a recovery of the Sahelian vegetation from the drought conditions of the 1970s and 1980s.

The second set of analyses specifically focused on the Sahel region and the variability in the vegetation seasonal course. From the ICA first mode, we derived a Sahelian NDVI index and determined high photosynthetic activity onset and cessation dates. These dates occur in the first 10-day period of July and the second 10-day period of November, respectively. The onset date follows by only 1 to 2 weeks the northward shift of the ITCZ and shows small interannual variations compared to the cessation date. The latter is characterized by a positive significant trend coherent with an increase of rainfall over the study period. A second step consisted of classifying years according to their vegetative seasonal cycle. Years of low (e.g., 1984, 1987) and high (e.g., 1994, 1999) photosynthetic activity show contrasted seasonal cycles: early versus delayed cessation, slow versus steep NDVI growth, and weak versus high NDVI levels. Specific rainfall courses are jointly observed. They feature below- versus above-normal rainfall amounts and a phase shifted toward July versus September. However, rainfall amounts are not the only factor governing the NDVI intraseasonal variability. The NDVI anomalies recorded at the green-up (i.e., June–July of year j) are mostly related to NDVI anomalies recorded for the previous vegetative season (i.e., NDVI maximum value of year $j - 1$). This finding supports the hypothesis of a year-to-year memory in vegetation already proposed in recent studies.

Acknowledgments. The authors are grateful to the CRU and to the UKMO for providing the rainfall data and the SST data, respectively, and to the FastICA team from the Computer and Information Science Laboratory (University of Technology, Helsinki) for providing a free software package of their FastICA algorithm. This study was supported by "ECCO-PNRH," a contribution to the French program "ACI-ECCO," as well as the European program "AMMA-6th PCRD." Based on a French initiative, AMMA was built as an international scientific group and is currently funded by a large number of agencies, especially from France, the United Kingdom, the United States, and Africa. AMMA has been the beneficiary of a major financial contribution from the European Community's Sixth Framework Research Programme. Detailed information on scientific coordination and funding is available on the AMMA International Web site, http://www.amma-international.org.

REFERENCES

Aires, F., A. Chédin, and J.-P. Nadal, 2000: Independent component analysis of multivariate time series: Application to the tropical SST variability. *J. Geophys. Res.,* **105,** 17 437–17 456.

——, W. B. Rossow, and A. Chédin, 2002: Rotation of EOFs by the independent component analysis: Toward a solution of the mixing problem in the decomposition of geophysical time series. *J. Atmos. Sci.,* **59,** 111–123.

Akpo, L. E., and M. Grouzis, 1993: Etude comparée de la phénologie de la végétation herbacée sous et hors couvert ligneux en milieu sahélien. *Webbia,* **47,** 387–401.

Anyamba, A., and J. R. Eastman, 1996: Interannual variability of NDVI over Africa and its relation to El Niño/Southern Oscillation. *Int. J. Remote Sens.,* **17,** 2533–2548.

——, and C. Tucker, 2005: Analysis of Sahelian vegetation dynamics using NOAA-AVHRR NDVI data from 1981–2003. *J. Arid Environ.,* **63,** 596–614.

Bader, J., and M. Latif, 2003: The impact of decadal-scale Indian Ocean sea surface temperature anomalies on Sahelian rainfall and the North Atlantic Oscillation. *Geophys. Res. Lett.,* **30,** 2169, doi:10.1029/2003GL018426.

Betts, A. K., J. H. Ball, A. C. M. Beljaars, M. J. Miller, and P. A. Viterbo, 1996: The land surface–atmosphere interaction: A review based on observational and global modeling perspectives. *J. Geophys. Res.,* **101,** 7209–7226.

Bonan, G. B., 2002: *Ecological Climatology: Concepts and Applications.* Cambridge University Press, 678 pp.

Camberlin, P., and N. Philippon, 2002: The East African March–

May rainy season: Associated atmospheric dynamics and predictability over the 1968–97 period. *J. Climate,* **15,** 1002–1019.

——, and M. Diop, 2003: Application of daily rainfall principal component analysis to the assessment of the rainy season characteristics in Senegal. *Climate Res.,* **23,** 159–169.

——, S. Janicot, and I. Poccard, 2001: Seasonality and atmospheric dynamics of the teleconnection between African rainfall and tropical sea-surface temperature: Atlantic vs. ENSO. *Int. J. Climatol.,* **21,** 973–1005.

Charney, J. G., 1975: Dynamics of desert and drought in the Sahel. *Quart. J. Roy. Meteor. Soc.,* **101,** 193–202.

Crépeau, C., and Coauthors, 2003: Monitoring of dry land area vegetation using products derived from satellite images. *Sécheresse,* **1E**. [Available online at http://www.secheresse.info/article.php3?id_article=224#.]

Dai, A., P. J. Lamb, K. E. Trenberth, M. Hulme, P. Jones, and P. Xie, 2004: The recent Sahel drought is real. *Int. J. Climatol.,* **24,** 1323–1331.

de Bie, S., P. Ketner, M. Paasse, and C. Geerling, 1998: Woody plant phenology in the West Africa savanna. *J. Biogeogr.,* **25,** 883–900.

Dregne, H. E., and C. J. Tucker, 1988: Green biomass and rainfall in semi-arid sub-Saharan Africa. *J. Arid Environ.,* **15,** 245–252.

Eklundh, L., and L. Olsson, 2003: Vegetation index trends for the African Sahel 1982–1999. *Geophys. Res. Lett.,* **30,** 1430, doi:10.1029/2002GL016772.

Eltahir, E. A. B., and C. Gong, 1996: Dynamics of wet and dry years in West Africa. *J. Climate,* **9,** 1030–1042.

Fontaine, B., and S. Janicot, 1996: Sea surface temperature fields associated with West African rainfall anomaly types. *J. Climate,* **9,** 2935–2940.

——, S. Trzaska, and S. Janicot, 1998: Evolution of the relationship between near global and Atlantic SST modes and the rainy season in West Africa: Statistical analyses and sensitivity experiments. *Climate Dyn.,* **14,** 353–368.

Fontès, J., J. P. Gastellu-Etchegorry, O. Amram, and G. Flouzat, 1995: A global phenological model of the African continent. *Ambio,* **24,** 297–303.

Giannini, A., R. Saravanan, and P. Chang, 2003: Oceanic forcing of Sahel rainfall on interannual to interdecadal time scales. *Science,* **302,** 1027–1030.

Grist, J., S. Nicholson, and A. Mpolokang, 1997: On the use of NDVI for estimating rainfall fields in the Kalahari of Bostwana. *J. Arid Environ.,* **35,** 195–214.

Hanan, N. P., S. D. Prince, and B. N. Holben, 1995: Atmospheric correction of AVHRR data for biophysical remote sensing of the Sahel. *Remote Sens. Environ.,* **51,** 306–316.

Hansen, M., R. DeFries, J. R. G. Townshend, M. Carroll, C. Dimiceli, and R. Sohlberg, 2002: Global percent tree cover at a spatial resolution of 500 meters: First results of the MODIS vegetation continuous fields algorithm. *Earth Interactions,* **7.** [Available online at http://EarthInteractions.org.]

Hiernaux, P. H. Y., M. I. Cissé, L. Diarra, and P. N. de Leeuw, 1994: Fluctuations saisonnières de la feuillaison des arbres et buissons sahéliens: Conséquences pour la quantification des ressources fourragères. *Rev. Elev. Med. Vet. Pays Trop.,* **47,** 117–125.

Holben, B. N., and Coauthors, 2001: An emerging ground-based aerosol climatology: Aerosol optical depth from AERONET. *J. Geophys. Res.,* **106,** 12 067–12 097.

Huete, A. R., and C. J. Tucker, 1991: Investigation of soil influences in AVHRR red and near-IR vegetation index imagery. *Int. J. Remote Sens.,* **12,** 1223–1242.

Hutjes, R. W. A., and Coauthors, 1998: Biospheric aspects of the hydrological cycle. *J. Hydrol.,* **212–213,** 1–21.

Hyvarinen, A., and E. Oja, 2000: Independent component analysis: Algorithms and applications. *Neural Networks,* **13,** 411–430.

——, J. Karhunen, and E. Oja, 2001: *Independent Component Analysis*. John Wiley and Sons, 481 pp.

Janicot, S., 1992: Spatiotemporal variability of West African rainfall. Part I: Regionalizations and typings. *J. Climate,* **5,** 489–497.

——, V. Moron, and B. Fontaine, 1996: Sahel droughts and ENSO dynamics. *Geophys. Res. Lett.,* **23,** 515–518.

——, S. Trzaska, and I. Poccard, 2001: Summer Sahel-ENSO teleconnection and decadal time scale SST variations. *Climate Dyn.,* **18,** 303–320.

Jarlan, L., Y. M. Tourre, E. Mougin, N. Philippon, and P. Mazzega, 2005: Dominant patterns of AVHRR NDVI interannual variability over the Sahel and linkages with key climate signals (1982–2003). *Geophys. Res. Lett.,* **32,** L04701, doi:10.1029/2004GL021841.

Justice, C. O., G. Dugdale, J. R. Townshend, A. S. Narracott, and M. Kumar, 1991: Synergism between NOAA-AVHRR and Meteosat data for studying vegetation development in semi-arid West Africa. *Int. J. Remote Sens.,* **12,** 1349–1368.

Le Barbé, L., T. Lebel, and D. Tapsoba, 2002: Rainfall variability in West Africa during the years 1950–90. *J. Climate,* **15,** 187–202.

Liebmann, B., and C. A. Smith, 1996: Description of a complete (interpolated) outgoing longwave radiation dataset. *Bull. Amer. Meteor. Soc.,* **77,** 1275–1277.

Los, S. O., G. J. Collatz, L. Bounoua, P. J. Sellers, and C. J. Tucker, 2001: Global interannual variations in sea surface temperature and land surface vegetation, air temperature, and precipitation. *J. Climate,* **14,** 1535–1549.

Lotsch, A., M. A. Friedl, and J. E. Pinzon, 2003: Spatio-temporal deconvolution of NDVI image sequences using independent component analysis. *IEEE Trans. Geosci. Remote Sens.,* **41,** 2938–2942.

Louvet, S., B. Fontaine, and P. Roucou, 2003: Active phases and pauses during the installation of the West African monsoon through 5-day CMAP rainfall data (1979–2001). *Geophys. Res. Lett.,* **30,** 2271, doi:10.1029/2003GL018058.

Malo, A. R., and S. Nicholson, 1990: A study of the rainfall and vegetation dynamics in the African Sahel using the normalized difference vegetation index. *J. Arid Environ.,* **19,** 1–24.

Martiny, N., P. Camberlin, and Y. Richard, 2005: Interannual persistence effects in vegetation dynamics of semi-arid Africa. *Geophys. Res. Lett.,* **32,** L24403, doi:10.1029/2005GL024634.

Mayaux, P., E. Bartholomé, S. Fritz, and A. Beward, 2004: A new land-cover map of Africa for the year 2000. *J. Biogeogr.,* **31,** 861–877.

Mitchell, T. D., T. R. Carter, P. D. Jones, M. Hulme, and M. G. New, 2004: A comprehensive set of high-resolution grids of monthly climate for Europe and the globe: The observed record (1901–2000) and 16 scenarios (2001–2100). Tyndall Center Working Paper 55, 30 pp.

Moulin, S., L. Kergoat, N. Viovy, and G. Dedieu, 1997: Global-scale assessment of vegetation phenology using NOAA/AVHRR satellite measurements. *J. Climate,* **10,** 1154–1170.

Myneni, R. B., S. O. Los, and C. J. Tucker, 1996: Satellite-based identification of linked vegetation index and sea surface tem-

perature anomaly areas from 1982–1990 for Africa, Australia and South America. *Geophys. Res. Lett.,* **23,** 729–732.

Nicholson, S., 2005: On the question of the "recovery" of the rains in the West African Sahel. *J. Arid Environ.,* **63,** 615–641.

——, M. Davenport, and A. R. Malo, 1990: A comparison of the vegetation response to rainfall in the Sahel and East Africa, using Normalized Difference Vegetation Index from NOAA AVHRR. *Climatic Change,* **17,** 209–241.

——, B. Some, and B. Kone, 2000: An analysis of recent rainfall conditions in West Africa, including the rainy seasons of the 1997 El Niño and the 1998 La Niña years. *J. Climate,* **13,** 2628–2640.

Olsson, L., L. Eklundh, and J. Ardö, 2005: A recent greening of the Sahel—Trends, patterns and potential causes. *J. Arid Environ.,* **63,** 556–566.

Philippon, N., and B. Fontaine, 2002: The relationship between the Sahelian and previous 2nd Guinean rainy seasons: A monsoon regulation by soil wetness? *Ann. Geophys.,* **20,** 575–582.

——, E. Mougin, L. Jarlan, and P.-L. Frison, 2005: Analysis of the linkages between rainfall and land surface conditions in the West African monsoon through CMAP, ERS-WSC, and NOAA-AVHRR data. *J. Geophys. Res.,* **110,** D24115, doi:10.1029/2005JD006394.

Pinzon, J., M. E. Brown, and C. J. Tucker, 2004: Satellite time series correction of orbital drift artifacts using empirical mode decomposition. *Hilbert-Huang Transform and Its Applications,* N. E. Huang and S. S. P. Shen, Eds., World Scientific, 167–186.

Raicich, F., N. Pinardi, and A. Navarra, 2003: Teleconnections between Indian monsoon and Sahel rainfall and the Mediterranean. *Int. J. Climatol.,* **23,** 173–186.

Rayner, N. A., D. E. Parker, E. B. Horton, C. K. Folland, L. V. Alexander, D. P. Rowell, E. C. Kent, and A. Kaplan, 2003: Global analyses of sea surface temperature, sea ice, and night marine air temperature since the late nineteenth century. *J. Geophys. Res.,* **108,** 4407, doi:10.1029/2002JD002670.

Rigina, O., and M. S. Rasmussen, 2003: Using trend line and principal component analysis to study vegetation changes in Senegal 1986–1999 from AVHRR NDVI 8 km data. *Dan. J. Geogr.,* **103,** 31–42.

Rowell, D. P., 2001: Teleconnections between the tropical Pacific and the Sahel. *Quart. J. Roy. Meteor. Soc.,* **127,** 1683–1706.

——, 2003: The impact of Mediterranean SSTs on the Sahelian rainfall season. *J. Climate,* **16,** 849–862.

Schwinning, S., and O. E. Sala, 2004: Hierarchy of responses to resource pulses in arid and semiarid ecosystems. *Oecologia,* **141,** 211–220.

——, ——, M. E. Loik, and J. R. Ehleringer, 2004: Thresholds, memory and seasonality: Understanding pulse dynamics in arid/semi-arid ecosystems. *Oecologia,* **141,** 191–193.

Servain, J., 1991: Simple climatic indices for the tropical Atlantic Ocean and some applications. *J. Geophys. Res.,* **96,** 15 137–15 146.

Shinoda, M., 1995: Seasonal phase lag between rainfall and vegetation activity in tropical Africa as revealed by NOAA satellite data. *Int. J. Climatol.,* **15,** 639–656.

——, and Y. Yamaguchi, 2003: Influence of soil moisture anomaly on temperature in the Sahel: A comparison between wet and dry decades. *J. Hydrometeor.,* **4,** 437–447.

Sultan, B., and S. Janicot, 2000: Abrupt shift of the ITCZ over West Africa and intra-seasonal variability. *Geophys. Res. Lett.,* **27,** 3353–3356.

Tanré, D., B. N. Holben, and Y. F. Kaufman, 1992: Atmospheric correction algorithm for NOAAAVHRR products: Theory and applications. *IEEE Trans. Geosci. Remote Sens.,* **30,** 231–248.

Tateishi, R., and M. Ebata, 2004: Analysis of phenological change patterns using 1982–2000 Advanced Very High Resolution Radiometer (AVHRR) data. *Int. J. Remote Sens.,* **25,** 2287–2300.

Townshend, J. R., and C. O. Justice, 1986: Analysis of the dynamics of African vegetation using the normalized difference vegetation index. *Int. J. Remote Sens.,* **7,** 1435–1445.

Tucker, C. J., 1979: Red and photographic infrared linear combinations for monitoring vegetation. *Remote Sens. Environ.,* **8,** 127–150.

——, 2005: An extended AVHRR 8-km NDVI data set compatible with MODIS and SPOT vegetation NDVI data. *Int. J. Remote Sens.,* **26,** 1461–1471.

Vizy, E. K., and K. H. Cook, 2001: Mechanisms by which Gulf of Guinea and eastern North Atlantic sea surface temperature anomalies can influence African rainfall. *J. Climate,* **14,** 795–821.

Von Storch, H., and F. W. Zwiers, 1999: *Statistical Analysis in Climate Research.* Cambridge University Press, 484 pp.

Wang, G., and E. A. B. Eltahir, 2000a: Role of vegetation dynamics in enhancing the low-frequency variability of the Sahel rainfall. *Water Resour. Res.,* **36,** 1013–1021.

——, and ——, 2000b: Ecosystem dynamics and the Sahel drought. *Geophys. Res. Lett.,* **27,** 795–798.

Wilks, D. S., 2006: *Statistical Methods in the Atmospheric Sciences.* 2d ed. Academic Press, 627 pp.

Xie, P., and P. Arkin, 1997: Global precipitation: A 17-year monthly analysis based on gauge observations, satellite estimates, and numerical model outputs. *Bull. Amer. Meteor. Soc.,* **78,** 2539–2558.

Xue, Y., 1997: Biosphere feedback on regional climate in tropical North Africa. *Quart. J. Roy. Meteor. Soc.,* **123,** 1483–1515.

Zeng, N. J., J. D. Neelin, K. M. Lau, and C. Tucker, 1999: Enhancement of interdecadal climate variability in the Sahel by vegetation interaction. *Science,* **286,** 1537–1540.

Zhang, X., M. A. Friedl, C. B. Schaaf, A. H. Strahler, and Z. Liu, 2005: Monitoring the response of vegetation phenology to precipitation in Africa by coupling MODIS and TRMM instruments. *J. Geophys. Res.,* **110,** D12103, doi:10.1029/2004JD005263.

Zheng, X., and E. A. B. Eltahir, 1998: The role of vegetation in the dynamics of West African monsoons. *J. Climate,* **11,** 2078–2096.